

Importance of Storage Power Plants (SPP) in Large-scale Renewable Energy Integration

Nayeemuddin Ahmed, Harald Weber
 Electrical Energy Supply (EEV)
 Institute for Electrical Power Engineering (IEE)
 University of Rostock
 Rostock, Germany
 {nayeemuddin.ahmed, harald.weber}@uni-rostock.de

Abstract—To achieve future climate targets and compensate for diminishing fossil fuel resources, an increasing amount of clean, renewable energy is needed as an alternative. Hence, during the past decade, there has been a rapid increase in the integration of such renewable resources, mainly solar and wind, to the current electrical grid. However, the energy from such sources is highly intermittent and at times can be completely unrelated to the demand in the electrical network. Hence, in an electrical grid powered mostly by renewables, i.e. via wind turbines and photovoltaics, there would be a significant difference between the instantaneous power generation and consumption. To bridge this gap, a feasible method of large-scale energy storage is required. The Storage Power Plant (SPP), which uses hydrogen as its primary fuel, is one such solution.

In this investigation, the proposed SPPs are part of an isolated network that contains conventional thermal and hydroelectric power plants along with a large share of wind farms. Two separate events are created, the first involving excess power generation from the wind farms and the second representing the shutdown of a coal-fired thermal power plant. The dynamic interaction of the SPPs with the other power plants and the roles of its internal components are analyzed in both cases. The results highlight that the principles of power system control which are satisfied today with thermal power plants running on coal can also be met by the SPPs in the future.

I. INTRODUCTION

Presently, 14.8% of Germany's gross final energy consumption (around 2500 TWh) originates from renewable energy sources (RES) [1]. The aim of the EU 2020 energy strategy is to raise this share to 18% with future targets projecting it to be around 60% by the year 2050 [2]–[4]. Such high penetration of RES (primarily wind and solar), although necessary, introduces additional challenges in ensuring stability and reliability of the electrical grid. The ever increasing infeed from these RES leads to higher frequency fluctuations, presence of harmonics, as well as increased forecast errors due to their intermittent nature [5].

The difference between the varying electrical energy generation from RES and consumption by loads leads to either an energy deficit or surplus in the grid. At present, conventional power plants (CPPs) have to compensate for this disparity. However, in the future, the number of these CPPs, especially coal fired power plants, will decrease drastically to fulfill energy sector targets [6]. Thus, Electrical Energy Storage (EES) systems are regarded as viable alternatives to compensate for the intermittent and decentralized RES, in order to meet the network demand at all times [7].

Depending on its principle an EES type has its pros and cons. Flywheels and supercapacitors have high charge and

discharge rates, but, due to their sizes, are impractical long-term energy storages [8]. In comparison to supercapacitors, battery energy storages have a higher energy density, but a much slower response [9]. Meanwhile, hydrogen storages can be used to supply or store large magnitudes of energy but, due to the rate of the electrochemical reactions in a fuel cell or electrolyser, have an even slower response. A combination of these elements, though, will not only compensate for the shortcomings of these individual storage types but also assist in exploiting their advantages. Hence, such an interconnected system is presented in this paper, called Storage Power Plant (SPP) [10].

The operation of a SPP in a futuristic electrical grid with nodal voltage angle control as ancillary service has been discussed before [11]–[13]. Then again, to be regarded as a suitable solution for the present scenario, the SPP needs to function coherently with CPPs and RES in a frequency governed grid. Hence, the goal of this paper is to show the dynamic interaction between these different types of power plants. The following section describes the electrical grid, which is used as the test environment for this study. This is followed by an explanation of the component chain present inside a SPP, focusing on the role of each element. The result section comprises of two parts where the response of these power plants is analyzed, firstly during a ramp increase in power generation from RES and secondly during the shutdown of a coal fired power plant. Finally, the highlights of the investigations are then summed up in the conclusion.

II. TEST ELECTRICAL NETWORK

The test bench for the investigations is shown in Fig. 1. The network consists of 25 equidistant nodes, each connected to either a power plant or a load. The nodes are interconnected via transmission lines, each 250 km long and at a voltage level of 110 kV. The line impedances are equal in magnitude with a resistance to reactance ratio of 0.1.

There are eleven power plants, of which five are slack SPPs (S), i.e. converters at terminals where the voltage magnitude ($|V|$) and angle (ϕ_u) are kept constant. Out of the other six, four represent wind power plants (W), while the other two each denote a conventional hydroelectric (H) and a coal fired thermal (T) power plant. The CPPs are represented by PV terminals, where the active power (P) and voltage magnitude ($|V|$) are controlled. The four wind power plants (WPPs) and remaining 14 nodes, each housing

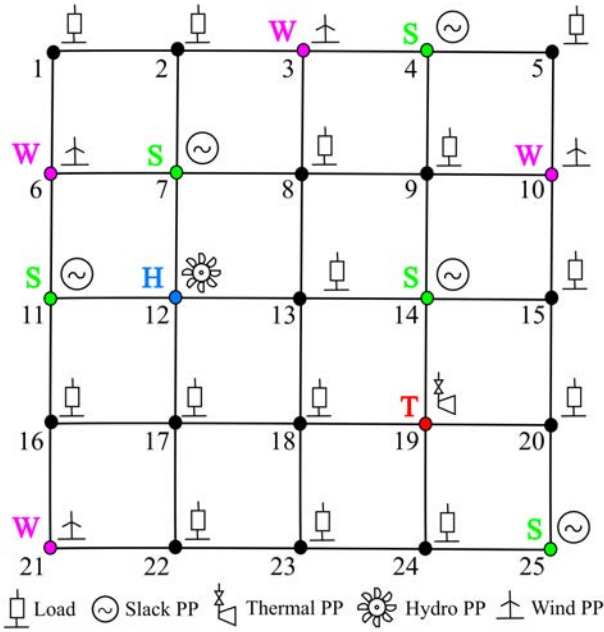


Fig. 1. 25 node electrical network

a load, are represented by PQ terminals where the active (P) and reactive power (Q) being consumed are known.

The network modeling and RMS simulations are carried out in the software DIGSILENT PowerFactory. The base power value of the per-unit-system is set as 10 MVA. The initial load flow setpoints for the loads and different power plants are summarized in Table I. Each load also consumes 1 MVAR of reactive power which is supplied by the power plants. Unfortunately, the reactive power results and control methods are not included in this paper due to space constraints.

III. INTERNAL SPP STRUCTURE

As seen in Fig. 2, the SPP consists of three main storages; the supercapacitor, battery and hydrogen storage. These storages have different energy capacities and are responsible for providing instantaneous reserve, primary and secondary

TABLE I

INITIAL WORKING POINTS OF DIFFERENT POWER PLANTS AND LOADS

Type	No.	Power per PP (MW)	Total power (MW)
Thermal power plant	1	10	10
Hydro power plant	1	10	10
Wind power plant	4	1	4
Storage power plant	5	4.742	23.71
Total Generation	-	-	47.71
Loads	14	3.4	47.6
Losses	-	-	0.11
Total Consumption	-	-	47.71

control respectively. There are DC-DC converters between the storages which control the power flow between them. All components operate in DC mode. Hence, the power plant uses a DC-AC converter for grid connection. The SPP structure used in the simulation software, models the control scheme of the DC-DC converters which govern the power flow between the SPP storage components. The components themselves are represented by simplified ideal models.

The first storage, i.e. the supercapacitor, is directly connected to the DC-AC grid converter. In case of a network disturbance, it immediately supplies instantaneous reserve to the grid or stores it from the grid. It can instantaneously charge and discharge with a high power gradient and additionally has an almost infinite lifetime because of its electrostatic storage principal. These properties make it ideal for its task of providing instantaneous response. Hence, its behavior is analogous to the rotating mass in a turbine shaft of a conventional thermal power plant (TPP).

The second storage, i.e. the battery, connected in parallel to the supercapacitor, supplies or stores primary control power, in order to compensate for the low power density of the supercapacitor. This process is controlled by the DC-DC converter between these two components. In contrast to a

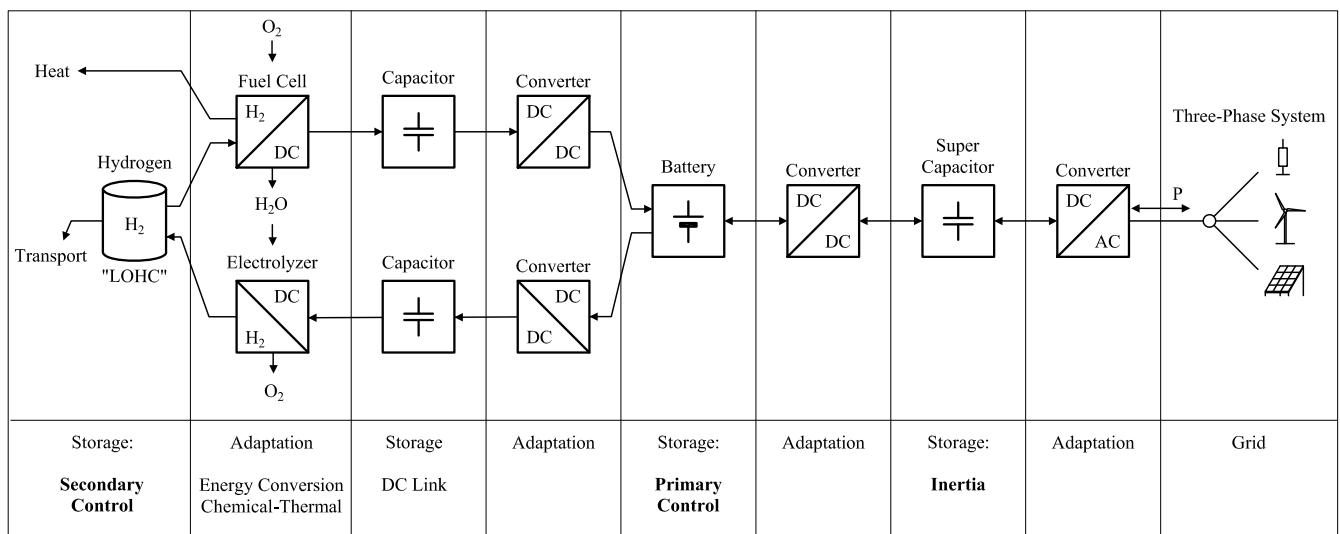


Fig. 2. Working principle of the internal components of a Storage Power Plant (SPP)

supercapacitor, the battery is optimally suited for the purpose of providing primary control power. This is due to its electrochemical energy storage principle which allows it to possess a higher energy storage density compared to a supercapacitor and a preferably lower charging and discharging gradient, to improve its lifetime. Thereby, it represents the equivalent of the steam boiler in a conventional TPP.

As the third main storage, the hydrogen storage is responsible for supplying secondary control power, similar to the coal storage in a coal fired TPP. Additionally, it can store secondary control power. Depending on the power flow direction, either a fuel cell or an electrolyser is used to empty or refill the hydrogen storage. The power flow for each of these cases is controlled by the DC-DC converter in the respective paths between the hydrogen storage and the battery. Each of these two DC-DC converters possesses a DC link buffer storage. The behavior of these capacitors is analogous to the steam boiler pipe wall in a TPP.

While utilizing the hydrogen storage, the fuel cell generates electrical energy from the chemical reaction between stored hydrogen (H_2) and external oxygen (O_2). One by-product of this reaction is thermal energy which can be used for district heating. Another product is dihydrogen monoxide (H_2O). In case of a reversed power flow, the H_2O can in turn be used as the electrolyte to generate hydrogen as well as oxygen as a by-product. The hydrogen can then be stored in a Liquid Organic Hydrogen Carrier (LOHC) system. Such a system enables safe, easy storage and transportation of hydrogen at a high energy density under ambient conditions, using the currently available infrastructure [14]. In addition to being used for electrical power generation in the SPP, the stored hydrogen can also be utilized in other applications, for example in automobiles.

IV. RESULTS AND OBSERVATION

To analyze the dynamic behavior of the SPP in combination with the other power plants, two separate investigations are performed. In the first case, the generation of all the WPPs in the 25 node network are ramped by equal magnitudes and the response of the other power plants to the presence of surplus power in the grid is examined. In the second case, the TPP is suddenly disconnected from the grid and the ancillary action of the other power plants to bridge the corresponding power deficit is investigated.

A. Study Case 1

The ramp to increase the power generation of the four WPPs exists between 100 s and 300 s, as shown in Fig. 3. This portrays a situation when the power output of the WPPs would increase steadily due to an increase in the wind speed. As a result, the output of each WPP increases from 1 MW to 10 MW, shown as pu values in Fig. 3. At the same time, the power output of the SPP, TPP and hydroelectric power plant (HPP) decreases to maintain the balance between generation and demand. The output of the TPP and HPP levels off at 5 MW (0.5 pu) since it should function at least at 50% of its nominal power to maintain feasible operation. This is compensated by the five SPPs which then start to reduce their power output at a faster rate. Such values are chosen for the WPP output ramp so that the power output of every

SPP reduces beyond zero and its energy storing ability can be studied. Due to this increase in power generation, the grid frequency rises steadily and reaches its peak value when the ramp ends, as shown in Fig. 4. After this time, the secondary controllers of the power plants take over significantly and return the frequency to its initial value of 1 pu.

Fig. 5a depicts that as soon as the ramp in WPP generation starts, the TPP, HPP and SPP outputs decrease. The reduction in the SPP power production consequently causes the output of the DC-AC converter, between the supercapacitor and the three-phase grid, to decrease as well. At the same time, the output of the DC-DC converter, between the battery and the supercapacitor, is slightly higher than that of the DC-AC converter. The resulting difference leads to a momentary surplus power flow into the supercapacitor causing it to charge and its voltage to rise, as shown in Fig. 5c. This represents the instantaneous response of the SPP, as provided by the supercapacitor.

The hydrogen mass flow from the SPP fuel cell is higher than the output of the DC-DC converter between the supercapacitor and battery. The resulting difference causes the battery to charge, signified by the first short negative dip in battery current in Fig. 5b. This represents the primary control response of the SPP, as provided by the battery. The corresponding battery voltage increases beyond the battery's lower threshold of 0.99 pu and this causes the DC-DC converter controlling the fuel cell to gradually reduce the fuel cell output to zero.

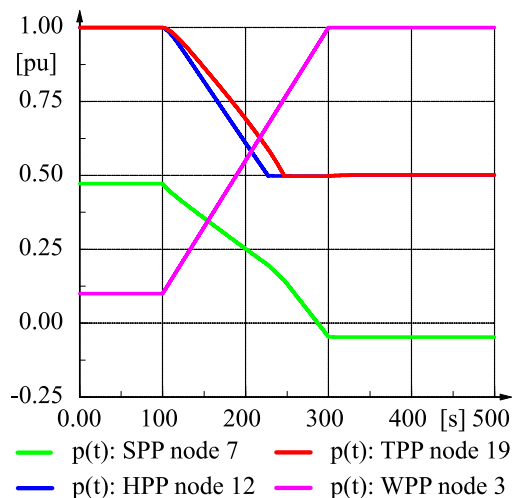


Fig. 3. Ramp increase in power generation by the WPPs with the corresponding response of the other types of power plants

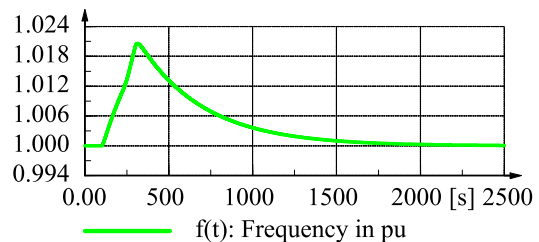


Fig. 4. Change in grid frequency due to the ramp increase in power generation by the WPPs

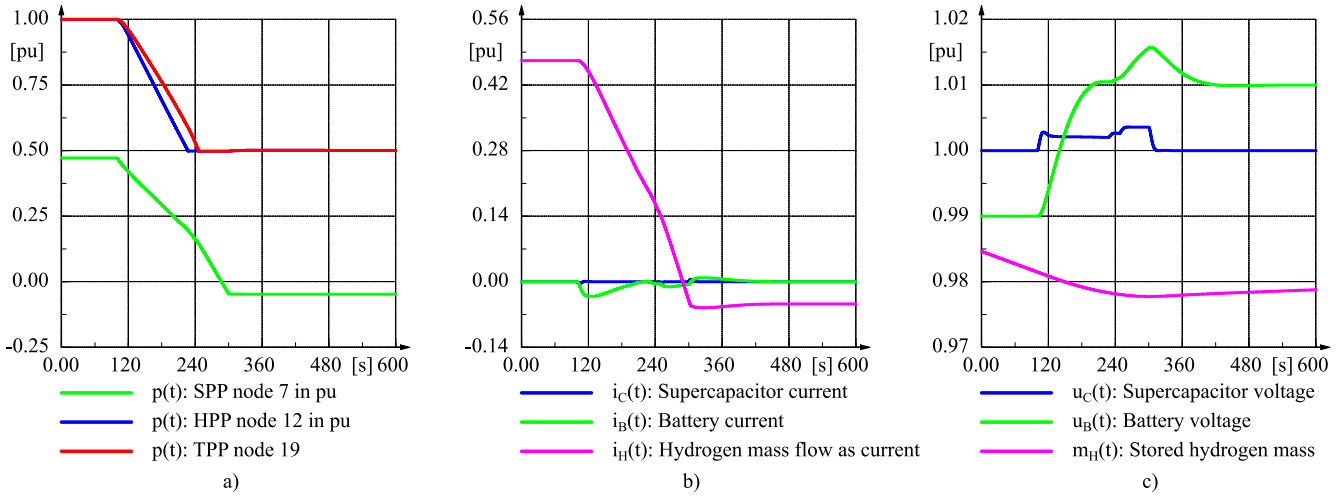


Fig. 5. a) Active power output of the three different types of power plants, b) Current from from the SPP storages and c) Voltage levels of the storages due to the ramp

Once the HPP and TPP reach their lower power output limit of 5 MW, the supercapacitor and battery inside the SPP gets charged again due to excess power arriving from the grid. Their corresponding voltage levels rise and when the battery voltage crosses its upper threshold of 1.01 pu, the DC-DC converter regulating the electrolyzer raises the converter output, increasing the hydrogen mass flow rate towards the hydrogen storage, as exhibited in Fig. 5b. Consequently, the stored hydrogen mass now starts to gradually increase, Fig 5c. When the ramp ends at 300 s, both the capacitor and battery are discharged by the regulating DC-DC converters to retain their voltage levels of 1 pu and 1.01 pu respectively. From then onwards, the energy storage of the SPP is only governed by its steady rate of hydrogen mass flow, denoting the action of secondary control response in the SPP.

B. Study Case II

The working points of the four different types of power plants are retained from the end points of the first case of investigation. This investigation depicts a futuristic scenario where the coal fired power plants would be shut down. Thus, in this situation, the coal fired TPP is disconnected from the

grid at 100 s and the effect of this sudden change on the dynamic behavior of the other three types of power plants is explored.

As soon as the TPP is shut off, its power output drops from 5 MW to 0 MW. The resulting power deficit causes the grid frequency to drop immediately, as displayed in Fig. 6. The rate of frequency change varies slightly for every node in the grid structure and is used by the respective power plants to provide their corresponding instantaneous reserve. The frequency deviation is used to provide primary control

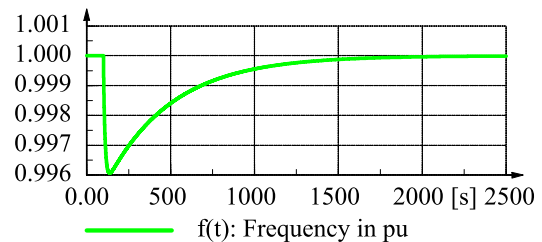


Fig. 6. Change in grid frequency due to shutting off the TPP

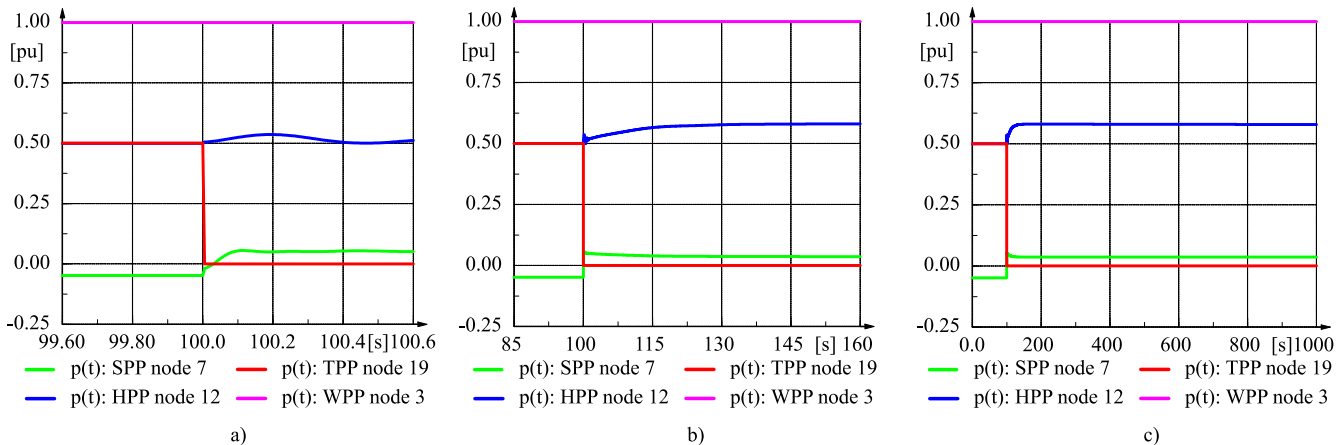


Fig. 7. a) Active power output of the four different types of power plants, b) Current from the SPP storages and c) Voltage levels of the storages due to disconnection of the TPP

power and once the secondary control power starts to flow, the frequency is returned to 1 pu.

The ancillary response of the other three types of power plants to the sudden power deficit is portrayed in Fig. 7. In these investigations, the WPPs are represented as converters operating at their constant rated power. Hence, they do not provide any ancillary service. Fig. 7a highlighting the instantaneous response of the different power plants exhibits that the SPP at node 7 reacts faster than the HPP and provides a slightly greater increase in active power output.

Fig. 7b displays the supplying of primary control power by the different power plants. The power output of the HPP rises gradually to its maximum value. Meanwhile, the output of the SPP decreases steadily so that the overall increase in power generation balances the power deficit in the network. Fig. 7c demonstrates the secondary control power flows, illustrating that the power output of the SPP and HPP increases almost by the same value. This is because both types of power plants have the same time constant for their secondary controller. However, the HPP

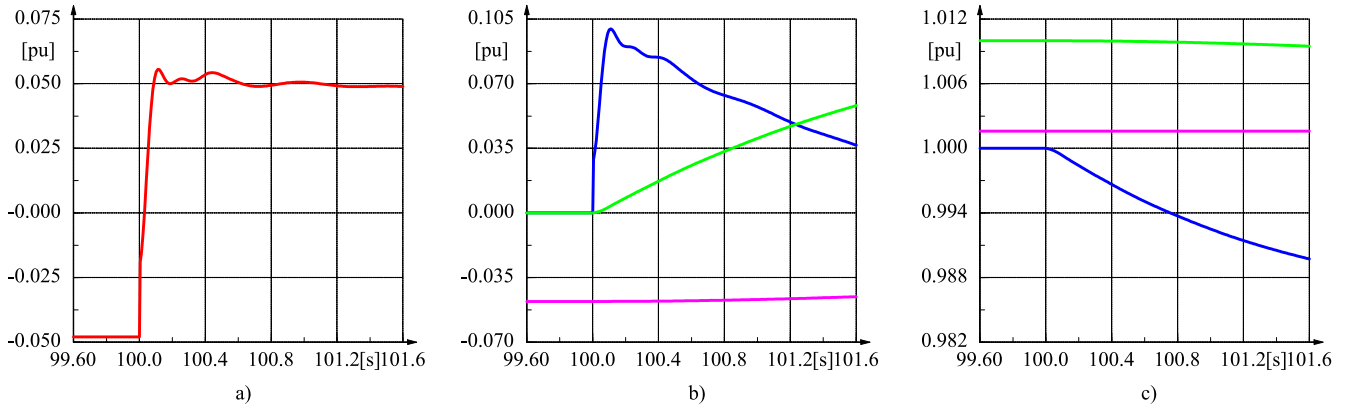


Fig. 8. a) Increase in power output, b) Current flow from the SPP storages and c) Voltage levels of the storages during the initial short time frame

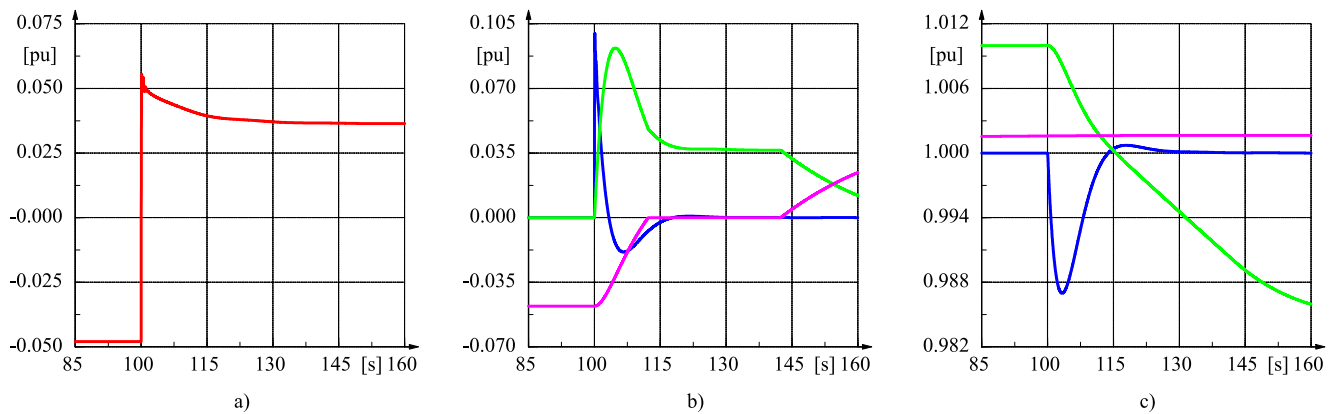


Fig. 9. a) Increase in power output, b) Current flow from the SPP storages and c) Voltage levels of the storages during the medium time frame

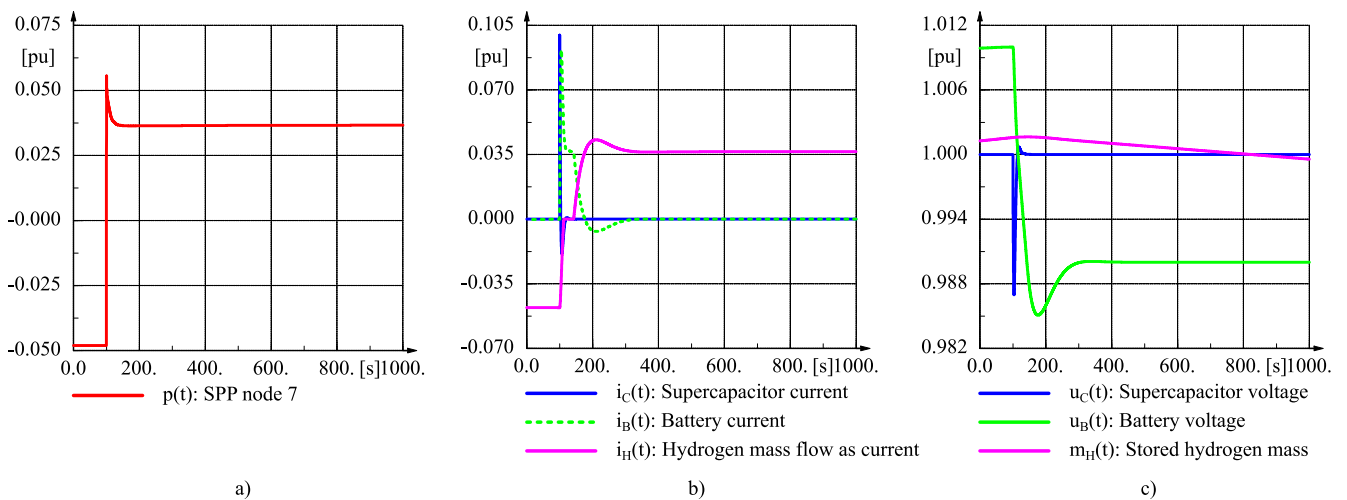


Fig. 10. a) Increase in power output, b) Current flow from the SPP storages and c) Voltage levels of the storages during the long time frame

has a slightly lower power output owing to the friction on its penstock walls.

Next, the behavior of the internal components of the SPP at node 7 is investigated to examine the power plant's ability to provide ancillary services. Fig. 8a shows the active power output of the SPP at node 7. Fig. 8b illustrates the currents out of the respective storages while Fig. 8c exhibits the resulting change in the voltage or mass levels of these three storages. These trends are presented in three time scales in Fig. 8-10, in order to highlight the regulating services provided by the SPP and the storages associated with each of the control powers.

1) *SPP Short Time Frame Response*: The graph in Fig. 8b shows that, like rotating masses in a TPP, the supercapacitor immediately starts to supply instantaneous reserve with the onset of the positive disturbance, so the SPP can meet the increased network demand. As a result, the supercapacitor voltage decreases, as displayed in Fig. 8c. To ensure that the supercapacitor is able to respond to further disturbances, the DC-DC converter between the supercapacitor and battery takes over supplying the disturbed network demand and subsequently recharges the supercapacitor to its nominal value, as shown in Fig. 9c. This recharging phase of the supercapacitor is visible in Fig. 9b, where the supercapacitor current is negative for some time, indicating that the current is flowing into the storage, thus raising its voltage level.

2) *SPP Medium Time Frame Response*: For the primary control, the DC-DC converter between the battery and the supercapacitor, only uses the energy stored in the battery. Therefore, to provide primary control response, the battery current increases and its voltage decreases, as shown in Fig. 9b and Fig. 9c. In addition, this DC-DC converter limits the battery current gradient to lower the stress on the storage device and in the process improves its lifetime.

The battery voltage operates within a defined voltage dead band under steady state conditions. When this voltage surpasses the lower threshold of 0.99 pu as displayed in Fig. 9c, the DC-DC converter on the upper branch between the battery and the fuel cell in Fig. 2, increases its power flow to the grid. This power flow from the fuel cell continues to increase until it fully supplies the disturbed network demand on its own. Furthermore, the converter recharges the battery in the long run and raises its voltage to be within permissible limits of the dead band. This supply of secondary control power can be seen in the form of increased hydrogen mass flow in Fig. 9b.

3) *SPP Long Time Frame Response*: In the longer time frame represented in Fig. 10c, the consequent decrease in the stored hydrogen mass is shown. During steady state operation the network demand is fully supplied by the secondary control response originating from the hydrogen storage alone. The supercapacitor and battery currents return to zero and their voltage levels are also restored to the corresponding setpoints. The SPP continues to output a constant active power owing to the steady rate of hydrogen mass flow, as shown in Fig. 10a and b.

V. ACKNOWLEDGMENT

This paper was made within the framework of the research project "Netz-Stabil" and financed by the European Social Fund (ESF/14-BM-A55-0025/16). It is part of the qualification program "Promotion of Young Scientists in Excellent Research Associations - Programme for Excellence in Research in Mecklenburg-Western Pomerania".

VI. CONCLUSION

This paper exhibited the ability of SPPs to function effectively with CPPs and RES in a 25 node frequency controlled grid. Inside this network, a disturbance was created initially by applying a ramp increase in the WPP output and then by shutting down the TPP in the grid. The corresponding dynamic responses of the CPPs and SPPs were investigated. It was shown that the SPP is able to provide necessary ancillary response in the form of instantaneous reserve, primary and secondary control to overcome the disturbance. These power flows inside the SPP are regulated by the respective DC-DC converters between these storages. Further research will be required to estimate the total losses as well as the market compatibility of this novel scheme and hence prepare a quantitative comparison in relation to the present system.

REFERENCES

- [1] World Energy Balances IEA. (2016) Total final consumption (TFC) by source germany 1990 - 2016. [Online]. Available: <https://www.iea.org/statistics?country=GERMANY&year=2016&category=Energy%20consumption&indicator=TFBySource&mode=chart&dataTable=BALANCES>
- [2] H. Weber, T. Hamacher, and T. Haase, "Influence of wind energy on the power station park and the grid," *IFAC Proceedings Volumes*, vol. 39, no. 7, pp. 59–64, 2006.
- [3] Vgb PowerTech, "Electricity generation facts and figures 2018–2019," p. 3, 2018.
- [4] Energiewende, "The energy of the future, fifth energy transition monitoring report," 2015.
- [5] X. Liang, "Emerging power quality challenges due to integration of renewable energy sources," *IEEE Transactions on Industry Applications*, vol. 53, no. 2, pp. 855–866, 2016.
- [6] German Institute for Economic Research, *Phasing out Coal in the German Energy Sector*. DIW Berlin, 2019.
- [7] H. Ibrahim, A. Ilinca, and J. Perron, "Energy storage systems — Characteristics and comparisons," *Renewable and sustainable energy reviews*, vol. 12, no. 5, pp. 1221–1250, 2008.
- [8] I. Hadjipaschalis, A. Poullikkas, and V. Efthimiou, "Overview of current and future energy storage technologies for electric power applications," *Renewable and sustainable energy reviews*, vol. 13, no. 6–7, pp. 1513–1522, 2009.
- [9] B. Dunn, H. Kamath, and J.-M. Tarascon, "Electrical energy storage for the grid: a battery of choices," *Science*, vol. 334, no. 6058, pp. 928–935, 2011.
- [10] H. Weber, "Von der frequenzregelung mit schwingmassen (netzstützende maßnahmen) zur winkelregelung mit umrichtern (netzbildende maßnahmen), from frequency control with inertia to angle control with converters."
- [11] H. Weber, P. Baskar, and N. Ahmed, "Power system control with renewable sources, storages and power electronic converters," in *2018 IEEE International Conference on Industrial Technology (ICIT)*. IEEE, 2018, pp. 1272–1278.
- [12] H. Weber, N. Ahmed, and P. Baskar, "Nodal voltage angle control of power systems with renewable sources, storages and power electronic converters," in *2018 International Conference on Smart Energy Systems and Technologies (SEST)*. IEEE, 2018, pp. 1–6.
- [13] —, "Power re-dispatch reduction with nodal voltage angle control in electrical energy supply systems," *IFAC-PapersOnLine*, vol. 51, no. 28, pp. 576–581, 2018.
- [14] D. Teichmann, W. Arlt, P. Wasserscheid, and R. Freymann, "A future energy supply based on liquid organic hydrogen carriers (LOHC)," *Energy & Environmental Science*, vol. 4, no. 8, pp. 2767–2773, 2011.